Characterization of Silicon Dioxide Films on a 4H-SiC Si(0001) Face by Fourier Transform Infrared (FT-IR) Spectroscopy and Cathodoluminescence Spectroscopy

MASANOBU YOSHIKAWA,* HIROHUMI SEKI, KEIKO INOUE, KEIKO MATSUDA, YUSAKU TANAHASHI, HIDEKI SAKO, YUIHIRO NANEN, MUNEHARU KATO, and TSUNENOBU KIMOTO

Toray Research Center Inc., Sonoyama 3-3-7, Otsu, Shiga 520-8567, Japan (M.Y., H.S., K.I., K.M., Y.T., H.S.); and Department of Electronic Science and Engineering, Kyoto University, A1-301 Katsura, Nishikyo, Kyoto 615-8510, Japan (Y.N., M.K., T.K.)

We used Fourier transform infrared (FT-IR) spectroscopy to characterize silicon dioxide (SiO_2) films on a 4H-SiC(0001) Si face. We found that the peak frequency of the transverse optical (TO) phonon in SiO_2 films grown on a 4H-SiC substrate agrees well with that in SiO_2 films grown on a Si substrate, whereas the peak frequency of the longitudinal optical (LO) phonon in SiO_2 films on a 4H-SiC substrate is red-shifted by approximately 50 cm^{-1} relative to that in SiO_2 films on a Si substrate. We concluded that this red-shift of the LO phonon is mainly caused by a change in inhomogeneity due to a decrease in density in the SiO_2 films. Furthermore, cathodoluminescence (CL) spectroscopy results indicated that the channel mobility of the SiC metal-oxide-semiconductor field-effect transistor (MOSFET) decreases roughly in proportion to the increase in the intensity of the CL peak at 460 and 490 nm, which is attributed to the increase in the number of oxygen vacancy centers (OVCs). FT-IR and CL spectroscopies provide us with a large amount of data on OVCs in the SiO_2 films on a 4H-SiC substrate.

Index Headings: **Characterization; Infrared spectroscopy; Fourier transform infrared spectroscopy; FT-IR spectroscopy; Cathodoluminescence spectroscopy; Silicon dioxide films; 4H-SiC Si(0001); Crystal defect.**

INTRODUCTION

Silicon carbide (SiC) is a well-known wide-bandgap semiconductor that contains native silicon dioxide (SiO_2), the presence of which makes it suitable for applications to high-power and high-frequency metal-oxide-semiconductor (MOS) devices. The interface trap densities (D_{it}) at the SiO_2/SiC interface and effective fixed charge density (Q_{eff}) are one to two orders of magnitude higher than those typically found at the SiO_2/Si interface (of the order of 10^{11} cm^{-2}),[1] and these degrade the channel mobility.[2–5] The presence of interface traps in SiC MOS field-effect transistors (FETs) is attributed to (i) excess carbon,[4,6] (ii) interface defects due to the presence of threefold coordinated O and C interstitial atoms,[4,6] and (iii) point defects such as Si and O vacancies that extend into the SiC underneath the SiO_2/SiC interface; this was determined via a comparison with SiO_2 films grown on a Si substrate.[7,8] Although post-oxidation annealing (POA) by H_2,[2] NO,[9,10] or N_2O[3,11–13] effectively increases the channel mobility, few studies have focused on changes induced by POA in the microstructure of SiO_2 films on SiC wafers.

Fourier transform infrared spectroscopy (FT-IR) is an effective tool for investigating chemical bonding structures in thin oxide films. In particular, the attenuated total reflection (ATR) configuration in infrared spectroscopy is a highly sensitive method for investigating surface-adsorbed species.[14] Transverse optical (TO) and longitudinal optical (LO) phonons were observed at around 1257 and 1072 cm^{-1}, respectively, in thermally grown SiO_2 films on a Si wafer.[8] These phonons are associated with the asymmetrical stretching of O in the inter-tetrahedral Si–O–Si bridge.[15] The peak frequency of these phonons is known to shift depending on factors such as the electromagnetic phase shift, inhomogeneity, densification, porosity, and SiO_2 film thickness. However, because these factors are interdependent, it is difficult to clarify the origin of the shift in TO and LO phonons. Although many studies have reported the FT-IR spectroscopy of thermally grown SiO_2 films on Si wafers, none have reported the same for SiC wafers.

Cathodoluminescence (CL) spectroscopy involves observing the luminescence that is produced when a sample is subjected to electron beam irradiation. This technique offers a higher spatial resolution than photoluminescence spectroscopy, the latter being based on visible laser beam irradiation.[16–18] CL spectroscopy provides considerable information about defects in thin SiO_2 films. In a previous study,[19] we measured the CL spectra of SiO_2 films on Si prepared by a variety of methods and observed peaks at 445 and 480 nm. A comparison of the CL and electron spin resonance (ESR) spectra of Si-doped quartz glass showed that these peaks originated from oxygen vacancy centers (OVCs), which differ from E′ centers. The CL measurement of the cross-section of a thermally grown SiO_2 film on a Si substrate indicated that the intensities of the abovementioned peaks in the SiO_2/Si interface were stronger than that of the CL peak at 640 nm that was attributed to non-bridging oxidation hole centers (NBOHCs).[17] However, we have never seen the CL spectra of SiO_2 films on a 4H-SiC wafer.

In this study, we investigated the origin of the peak shifts observed in TO and LO phonons in thermally grown SiO_2 films on a 4H-SiC(0001) Si face, compared the CL and FT-IR spectra of SiO_2 films grown on the 4H-SiC(0001) Si face, and clarified the relation between the microstructure of SiO_2 films and their electronic properties.

EXPERIMENTAL

Sample. Epitaxial layers with a thickness of approximately 5 μm were grown by chemical vapor deposition (CVD) on a 4° off-axis 4H-SiC(0001) Si face.[20] After RCA cleaning, thermal oxidation was carried out in dry O_2 at 1150 to 1300 °C, followed by POA in N_2O or NO atmosphere at 1300 °C. The

---

Received 15 November 2010; accepted 26 January 2011.

* Author to whom correspondence should be sent. E-mail: masanobu_yoshikawa@trc.toray.co.jp.

DOI: 10.1366/10-06186

0003-7028/11/6505-0543$2.00/0

Table I. Thickness, oxidation conditions, D_{it}, Q_{eff}, and channel mobility of thermally grown SiO_2 films on the 4H-SiC(0001) Si face.

	Thickness (nm)	Thermal oxidation	Post-oxidation	D_{it} (cm^{-2}) (Ec-0.2 ev)	Q_{eff} (cm^{-2})	Mobility (cm^2/Vs)
No. 1	59 nm	1150 °C 12 h.	N_2O anneal 1300 °C 120 min., Ar anneal 1300 °C 30 min.	5×10^{11}	-8×10^{11}	24
No. 2	58 nm	1150 °C 12 h.	N_2O anneal 1300 °C 120 min., Ar anneal 1300 °C 5 h.	5×10^{11}	-2×10^{11}	34
No. 3	55 nm	1300 °C 80 min.	NO anneal 1300 °C 80 min., Ar anneal 1300 °C, 30 min.	3×10^{11}	-2×10^{11}	38

samples were then annealed in Ar at 1300 °C. The oxide thickness was measured by ellipsometry. The typical oxide thickness was 55–59 nm. D_{it} was estimated from high-frequency (1 MHz) and low-frequency (quasi-static) C-V curves of n-type MOS capacitors, and Q_{eff} of the samples was determined from the flatband voltage in the C-V curves. The voltage sweep rate in C-V measurements was 0.1 V/s. The thickness, oxidation conditions, D_{it}, Q_{eff}, and channel mobility of the samples are listed in Table I.

Setup. Fourier transform infrared spectra were measured by a single-reflection attenuated total reflection (ATR) attachment in a Fourier transform spectrometer (Bruker IFS 66V). The incident angle was fixed at 60°, and a Ge crystal was used as an internal reflection element. The air gaps between the Ge prism and the samples were not controlled. We used a scanning electron microscope (SEM) with a Schottky-emission-type gun (HITACHI S-4300SE) as the excitation source for the CL measurement. The CL spectra were recorded using a Jobin Yvon HR-320 single monochromator equipped with a 1024-channel charge-coupled device (CCD) detector. We recorded the CL spectra at acceleration voltages of 3 and 5 kV at room temperature with a beam current of less than 5 nA. The electron beam was focused with an incident beam diameter of less than 10 nm. To minimize the degradation caused by electron beam irradiation, most CL spectra were measured for a period of 60 s. We repeated the CL measurement of each film two times and reproducible CL spectra were obtained.

RESULTS AND DISCUSSION

Figures 1a and 1b show FT-IR spectra of SiO_2 films on the 4H-SiC substrate. TO and LO phonons were observed at around 1205 and 1072 cm^{-1}, respectively. These modes are associated with the asymmetrical stretching of O in the inter-tetrahedral Si–O–Si bridge. Surprisingly, the peak frequency of the LO phonon in the SiO_2 films on a 4H-SiC substrate was red-shifted by approximately 50 cm^{-1} relative to that in typical thermally grown SiO_2 films on a Si substrate, whereas the peak frequency of the TO phonon in the SiO_2 films on the 4H-SiC substrate agreed well with that in SiO_2 films on a Si substrate.

The peak frequency of LO and TO phonons is generally considered to be affected by the following factors: (1) change in thickness,[21] (2) electromagnetic phase shifts,[22,23] (3) image charge effects,[23] (4) relaxation of stresses,[19] (5) densification,[21] and (6) inhomogeneity[21] (or porosity[24] or defects). The peak frequency of TO and LO phonons in the SiO_2 films has been reported to decrease with thickness.[21] Because all samples had similar thicknesses, factor (1) can be ignored. Martinet and Devine[22] simulated the frequency dependence of TO and LO phonons on the thickness with electromagnetic phase shifts. They found that the TO phonon exhibited a red-shift with a decrease in thickness, whereas the LO phonon essentially did

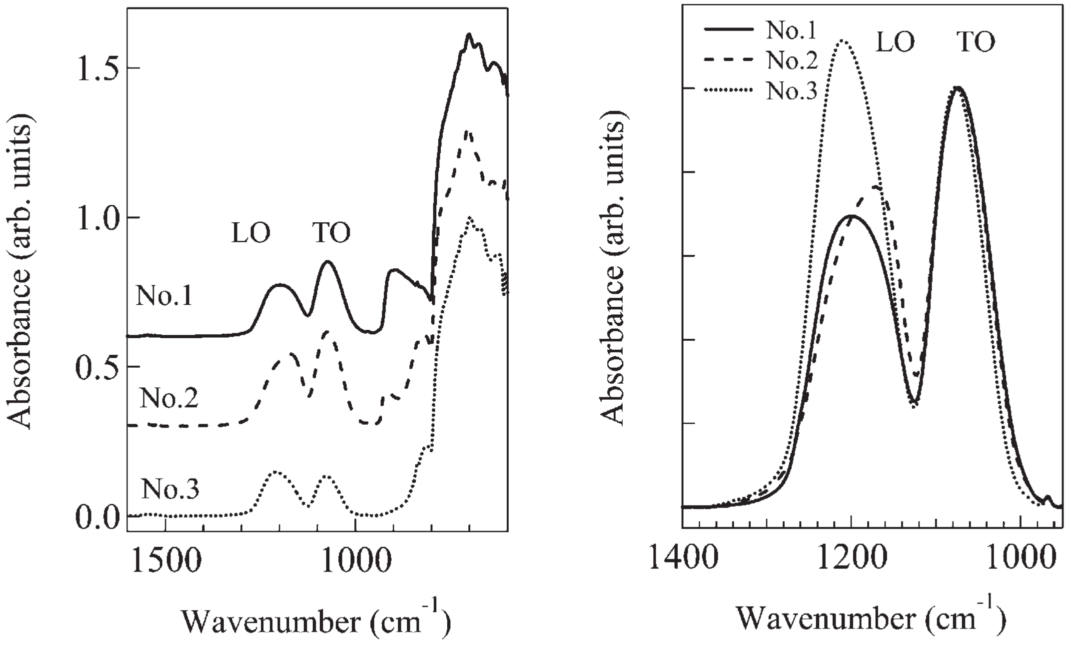

(a) (b)

FIG. 1. FT-IR spectra of SiO_2 films on the 4H-SiC(0001) Si face: (**a**) from 600 to 1600 cm^{-1} and (**b**) from 750 to 1400 cm^{-1}.

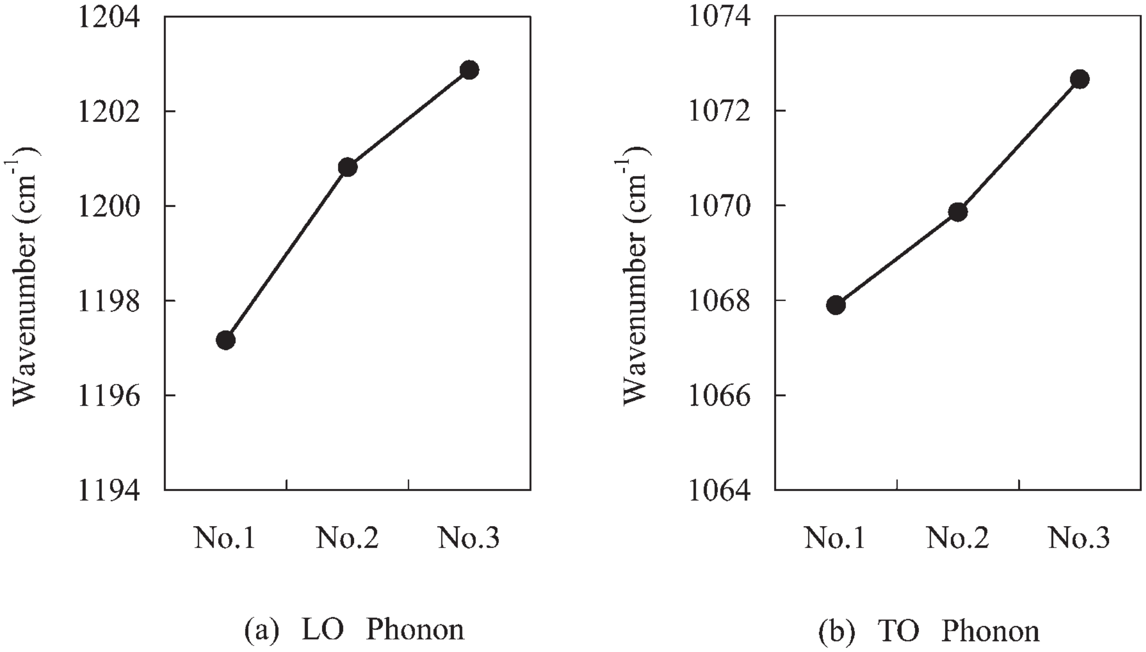

(a) LO Phonon

(b) TO Phonon

FIG. 2. Peak frequency shift of LO and TO phonons in the samples: (**a**) LO phonon and (**b**) TO phonon.

not. Hence, the peak-frequency shift observed for the LO phonon in the SiO_2 films cannot be explained by factor (2). Queeney et al.[23] calculated the red-shift of the LO phonon for a thin SiO_2 film on a Si substrate from the image charge effects and found that the image charge effects yielded a large red-shift of the LO phonon only in SiO_2 films with a thickness less than 1 nm; therefore, factor (3) is also excluded.

Generally, both TO and LO phonons shift to higher and lower frequencies under compressive and tensile stresses, respectively. The SiO_2 films were subjected to compressive stresses caused by a difference in thermal expansion coefficients between Si(SiC) and SiO_2 when the wafer was cooled from the deposition temperature to room temperature. As shown in Fig. 1, the peak frequency of the TO phonon in the SiO_2 films on the 4H-SiC substrate agrees well with that in SiO_2 films on the Si substrate, whereas the peak frequency of the LO phonon in the SiO_2 films on the 4H-SiC substrate was red-shifted by approximately 50 cm^{-1} relative to that in SiO_2 films on the Si substrate. This result cannot be explained by factor (4).

Nagai et al.[8,25] measured the FT-IR spectra of a SiO_2 film on a Si substrate prepared by thermal oxidation with gradient etching preparation and compared the density distributions of the SiO_2 film as calculated by grazing incidence X-ray reflectometry (GIXR). We carried out GIXR measurements of the density of the thermally grown SiO_2 film prepared under the same conditions as those for sample 1 before N_2O annealing. We found that the density of the sample was approximately 2.27 g/cm^3 and this was less than that of the SiO_2 film on a Si substrate (2.33 g/cm^3 in Ref. 25). This discussion may suggest that the 50 cm^{-1} red-shift of LO phonons in the SiO_2 films on the 4H-SiC substrate can be attributed to factor (5).

Queeney et al. simulated the FT-IR spectra of SiO_2 films on a Si substrate using effective medium approximation (EMA).[23] The FT-IR spectra of our samples roughly agreed with those calculated by EMA for a mixture of 65% silicon monoxide (SiO) and 35% SiO_2. The theoretical density of SiO bulk is 2.24.[26] Using the density of 2.24 for SiO bulk and the density of 2.33 g/cm^3 for typical SiO_2 films on a Si substrate,[25] we can roughly estimate that the average density of our sample is 2.27 g/cm^3 for a mixture of 65% SiO and 35% SiO_2. This value corresponded approximately with our result obtained from GIXR measurements. Furthermore, Queeney et al. found that both LO and TO phonons shifted to lower frequencies, and the red-shift of the LO phonon was more pronounced than that of the TO phonon. Based on their result and our result by GIXR measurements, the difference between the FT-IR spectra of SiO_2 films on Si and SiC substrates is considered to originate from a change in the inhomogeneity (this is probably due to defects in the SiO_2 films) due to a change in the density of SiO_2.

The peak-frequency shifts of LO and TO phonons in the samples are shown in Figs. 2a and 2b, respectively. The peak frequencies of LO and TO phonons were obtained by fitting a Gaussian curve to the spectrum shown in Fig. 1b. Because the LO phonon shown in Fig. 1b has an asymmetric line shape for sample 2, the LO phonon was fitted with two Gaussian curves at 1201 and 1155 cm^{-1}.

As shown in Figs. 2a and 2b, the peak frequencies of the TO and LO phonons shifted to increasingly lower frequencies from sample 3 to sample 1. On the other hand, the low-frequency part of the LO phonon divided into two components for sample 2 was observed at 1155 cm^{-1}. We measured the FT-IR spectra of a thermally grown SiO_2 film prepared under the same conditions as those for sample 1 before N_2O annealing and found that the LO and TO phonons were observed at approximately 1195 and 1072 cm^{-1}, respectively. The LO phonon was found to have a symmetric line shape, and the peak frequency of the LO phonon shifted to a lower frequency than that of samples 1 and 2. Furthermore, based on the results showing that the POA annealing time in Ar ambient (Table I) was too long for sample 2, the low-frequency part of the LO phonon observed at around 1155 cm^{-1} may originate from

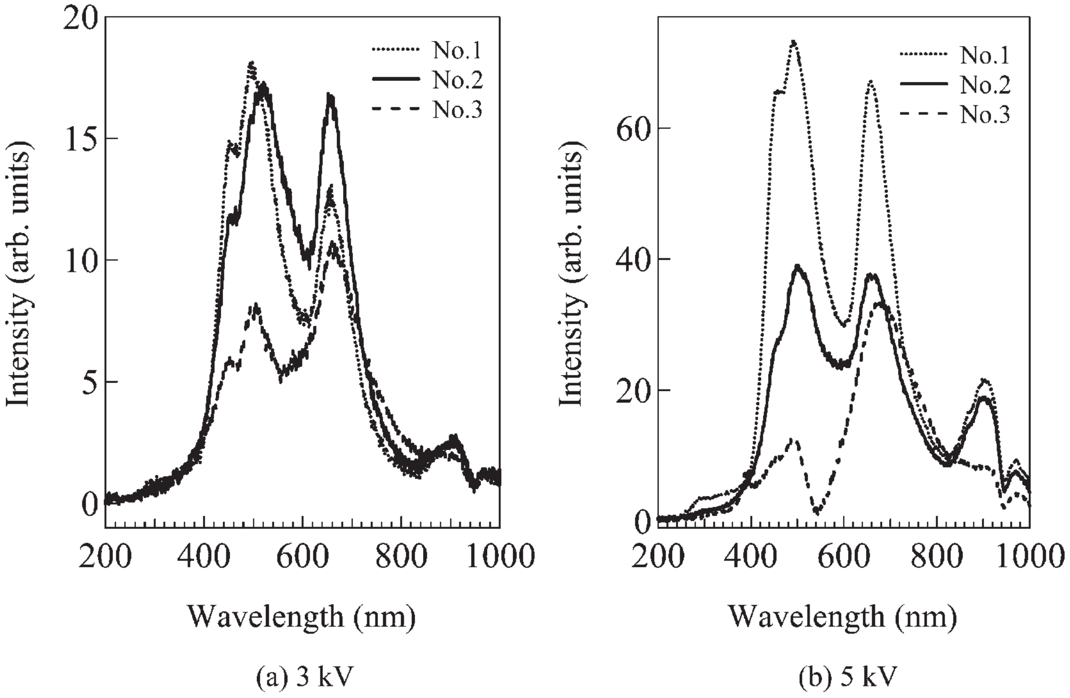

(a) 3 kV (b) 5 kV

FIG. 3. CL spectra of the samples measured at acceleration voltages of (**a**) 3 kV and (**b**) 5 kV.

Si–O–C, Si–N, and/or Si–O–N bonds formed by Ar annealing in the vicinity of the SiO_2/SiC interface.

Figures 3a and 3b show the CL spectra of the samples measured at acceleration voltages of 3 and 5 kV, respectively. CL peaks were observed at 460, 490, and 660 nm in the SiO_2 films on the 4H-SiC substrate. In the previous study,[19] we measured the CL spectra of SiO_2 films prepared by various methods and observed CL peaks at 445 and 480 nm. A comparison of the CL and ESR spectra of Si-doped quartz glass showed that the peaks at 460 and 490 nm originated from OVCs, which differ from E′ centers. The CL peak at 660 nm is usually attributed to the NBOHCs or their precursors.[27] As shown in Figs. 3a and 3b, the CL peaks at 460, 490, and 660 nm became increasingly intense from sample 3 to sample 1. This result indicates that the number of OVCs and NBOHCs increases from sample 3 to sample 1.

Figures 4a through 4c show the relation between the peak frequency of the LO phonon and the intensity of the CL peaks at 460, 490, and 660 nm, respectively. As shown in these figures, the peak frequency of the LO phonon decreases with an increase in the intensity of the CL peaks at 460 and 490 nm when measured at an acceleration voltage of 5 kV, whereas it does not strongly depend on the intensity of the CL peaks at 460 and 490 nm when measured at an acceleration voltage of 3

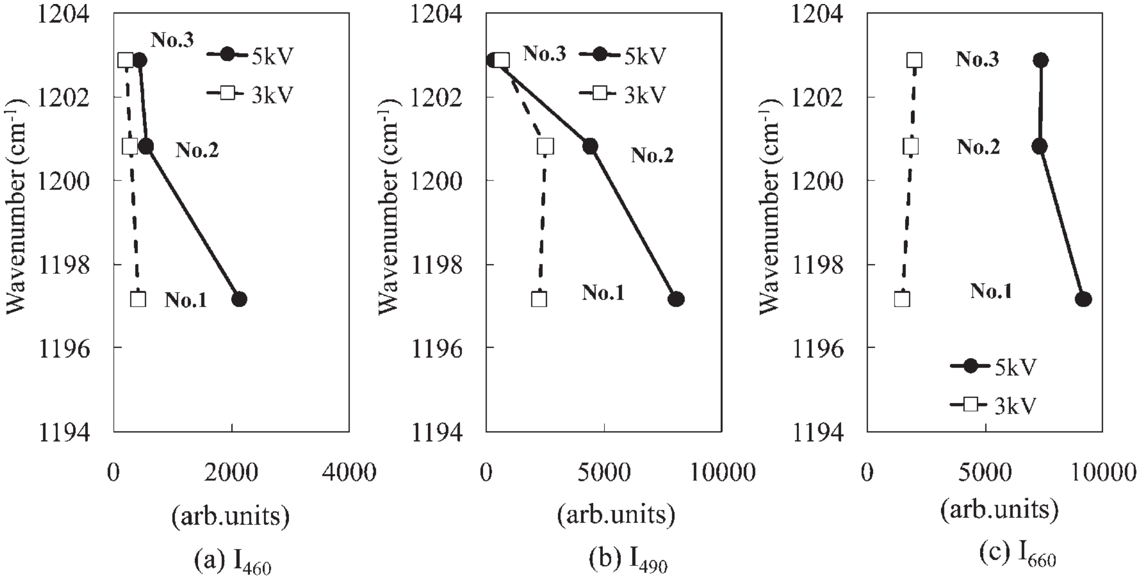

(a) I_{460} (b) I_{490} (c) I_{660}

FIG. 4. Relation between the peak frequency of the LO phonon and the CL integrated intensities at (**a**) 460, (**b**) 490, and (**c**) 660 nm.

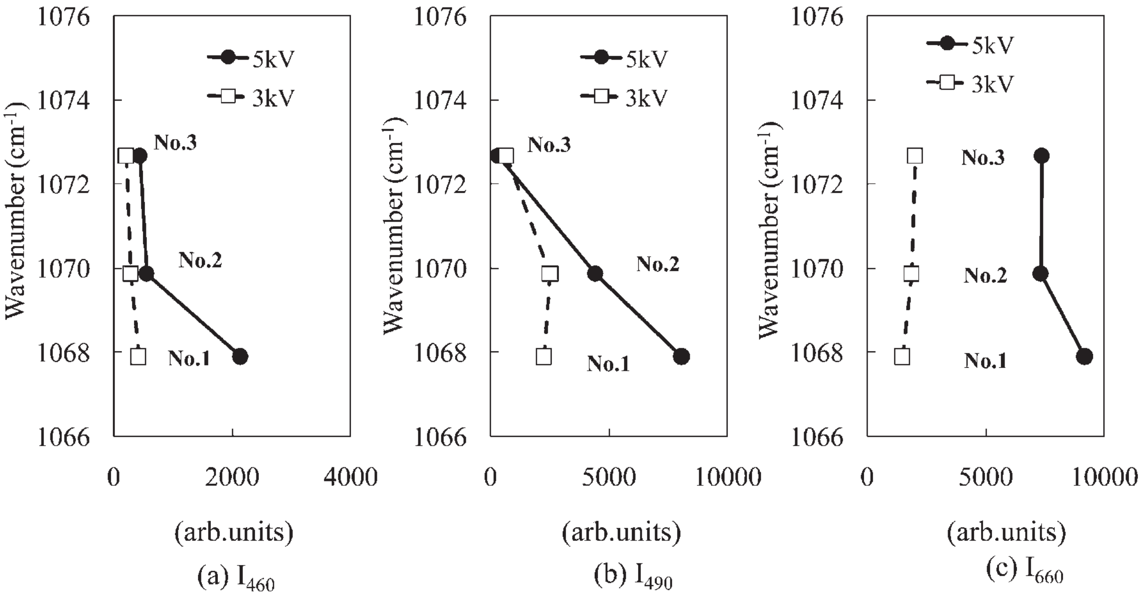

FIG. 5. Relation between the peak frequency of the TO phonon and the CL integrated intensities at (**a**) 460, (**b**) 490, and (**c**) 660 nm.

kV. Furthermore, the peak frequency of the LO phonon does not strongly depend on the intensity of the CL peak at 660 nm when measured at acceleration voltages of both 3 and 5 kV. This implies that the red-shift of the LO phonon is mainly attributable to an increase in the OVC content.

Figures 5a through 5c show the relationship between the peak frequency of the TO phonon and the CL peak intensities at 460, 490, and 660 nm, respectively. As shown in these figures, the peak frequency of the TO phonon decreases as the intensity of the CL peaks at 460 and 490 nm when measured at an acceleration voltage of 5 kV increases, whereas it does not strongly depend on the intensity of the CL peaks at 460 and 490 nm when measured at an acceleration voltage of 3 kV. Furthermore, the peak frequency of the TO phonon does not strongly depend on the intensity of the CL peak at 660 nm when measured at acceleration voltages of both 3 and 5 kV. This implies that the red-shift of the TO phonon is mainly attributable to an increase in the OVC content.

As shown in Figs. 4 and 5, the red-shift of the LO phonon is slightly larger than that of the TO phonon. This result is consistent with the simulation results obtained by Queeney et al. The comparison between the peak frequencies of the phonons and the CL peak intensities might indicate that a change in the inhomogeneity due to a decrease in the density of SiO_2 films is mainly caused by an increase in the OVC content in the SiO_2 films.

Monte Carlo simulations indicated that the penetration depths of electrons in thin SiO_2 films at acceleration voltages

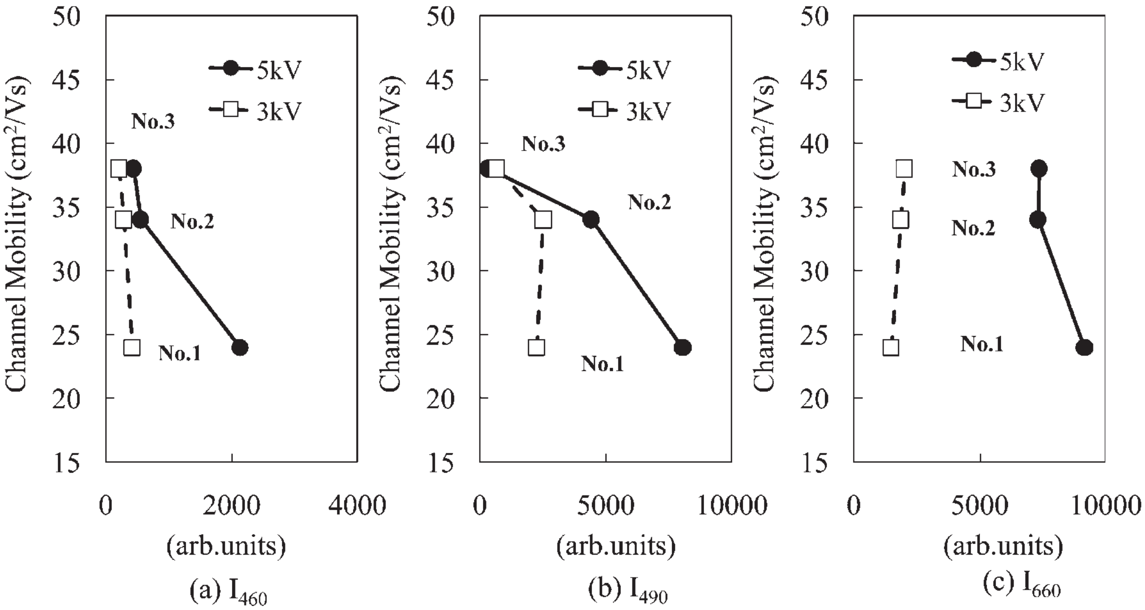

FIG. 6. Relation between the SiC-MOSFET channel mobility and the CL integrated intensities at (**a**) 460, (**b**) 490, and (**c**) 640 nm.

of 3 and 5 kV were approximately 30 and 60 nm, respectively. By comparing the penetration depth and sample thickness, the OVC content was found to increase in the vicinity of the SiO_2/SiC interface.

Figures 6a through 6c show the relation between the channel mobility of the SiC-MOSFET and the CL peak intensities at 460, 490, and 660 nm, respectively. As shown in these figures, the channel mobility decreases roughly in proportion to the increase in the intensity of the CL peaks at 460 and 490 nm when measured at an acceleration voltage of 5 kV, whereas it does not strongly depend on the intensity of the CL peaks at 460 and 490 nm when measured at an acceleration voltage of 3 kV. Furthermore, the channel mobility does not strongly depend on the intensity of the CL peak at 660 nm. These results suggest that the decrease in the channel mobility is mainly caused by an increase in the number of OVCs in the vicinity of the SiO_2/SiC interface. This shows that a decrease in the OVC content in the vicinity of the SiO_2/SiC interface effectively increases the channel mobility of the SiC-MOSFET. Furthermore, a comparison of the data presented in Table I and Fig. 6 indicates that an increase in the number of OVCs and NBOHCs is attributable to increases in not only the channel mobility but also in D_{it} and Q_{eff}. This may imply that high D_{it} and Q_{eff} in the SiO_2 films on SiC substrates is also mainly caused by the formation of OVCs and NBOHCs.

CONCLUSION

We measured the FT-IR and CL spectra of SiO_2 films grown on 4H-SiC wafers. We found that the peak frequency of TO phonons in SiO_2 films when grown on the 4H-SiC(0001) Si face agrees well with that in SiO_2 films grown on Si substrates, whereas the peak frequency of LO phonons in SiO_2 films grown on a 4H-SiC substrate is red-shifted by approximately 50 cm^{-1} relative to that in SiO_2 films on a Si substrate. We concluded that the red-shift of the LO phonon in the SiO_2 films on a 4H-SiC substrate is mainly caused by a change in the inhomogeneity due to a change in the density of SiO_2. Furthermore, the peak frequencies of the LO and TO phonons and CM of the SiC-MOSFET decrease roughly in proportion to the increase in the intensity of the CL peaks at 460 and 490 nm when measured at an acceleration voltage of 5 kV. This suggests that a decrease in the peak frequencies of these phonons and CM is mainly caused by an increase in the number of OVCs in the vicinity of the SiO_2/SiC interface. It was found that the channel mobility can be effectively increased by decreasing the OVC content in the vicinity of the SiO_2/SiC interface. FT-IR and CL spectroscopies provide us with a large amount of data on OVCs in the SiO_2 films on a 4H-SiC substrate.

---

1. S. M. Sze, *Semiconductor Devices, Physics and Technology* (John Wiley & Sons, 2002), 2nd ed., Chap. 6, p. 182.
2. K. Fukuda, M. Kato, K. Kojima, and J. Senzaki, Appl. Phys. Letts. **84,** 2088 (2004).
3. T. Kimoto, Y. Kanzaki, M. Noborio, H. Kawano, and H. Matsunami, Jpn. J. Appl. Phys. **44,** 1213 (2005).
4. V. V. Afanasev, M. Bassler, G. Pensl, and M. Schulz, Phys. Status Solidi A **162,** 321 (1997).
5. J. A. Cosper, Jr., Phys. Status Solidi A **162,** 305 (1997).
6. T. Zheleva, A. Lelis, G. Duscher, F. Liu, I. Levin, and M. Das, Appl. Phys. Lett. **93,** 022108 (2008).
7. T. Y. Luo, M. Laughery, G. A. Brown, H. N. Al-Shareef, V. H. C. Watt, A. Karamcheti, M. D. Jackson, and H. R. Huff, Electron Device Letters **21,** 382 (2000).
8. N. Nagai, K. Terada, Y. Muraji, H. Hashimoto, T. Maeda, Y. Maeda, E. Tahara, N. Tokai, and A. Hatta, J. Appl. Phys. **87,** 4747 (2002).
9. G. Y. Chung, C. C. Tin, J. R. Williams, K. McDonald, R. K. Chanana, R. A. Weller, S. T. Pantelides, L. C. Feldman, O. W. Holland, M. K. Das, and J. W. Palmour, IEEE Electron Device Lett. **22,** 176 (2001).
10. P. Jamet, S. Dimitrijer, and P. Tanner, J. Appl. Phys. **90,** 5058 (2001).
11. L. A. Lipkin, M. K. Das, and J. W. Palmour, Mater. Sci. Forum **389–393,** 985 (2002).
12. Y. Kanzaki, H. Kinbara, H. Kosugi, J. Suda, T. Kimoto, and H. Matsunami, Mater. Sci. Forum **457–460,** 1429 (2004).
13. M. K. Das, Mater. Sci. Forum **457–460,** 1275 (2004).
14. M. Yoshikawa and N. Nagai, *Handbook of Vibrational Spectroscopy*, J. M. Chalmers and P. R. Griffiths, Eds. (Wiley, Chichester, 2002), p. 2593.
15. F. L. Galeener, R. A. Barrio, E. Martinez, and R. J. Elliott, Phys. Rev. Lett. **17,** 2429 (1984).
16. R. G. Yacobi and D. B. Holt, *Cathodoluminescence Microscopy of Inorganic Solids* (Plenum Press, New York and London, 1990).
17. M. Yoshikawa, K. Iwagami, and H. Ishida, J. Appl. Phys. **51,** 1693 (1998).
18. M. Yoshikawa, M. Murakami, H. Ishida, and H. Harima, Appl. Phys. Lett. **94,** 131908 (2009).
19. M. Yoshikawa, K. Matsuda, Y. Yamaguchi, T. Matsunobe, Y. Nagasawa, H. Fujino, and T. Yamane, J. Appl. Phys. **92,** 7153 (2002).
20. T. Kimoto, A. Itoh, and H. Matsunami, Phys. Status Solidi B **202,** 247 (1997).
21. R. A. B. Devine, Appl. Phys. Lett. **68,** 3108 (1996).
22. C. Martinet and R. A. B. Devine, J. Appl. Phys. **77,** 4343 (1995).
23. K. T. Queeney, M. K. Weldon, J. P. Chang, Y. J. Chabal, A. B. Gurevich, J. Sapjeta, and R. L. Opila, J. Appl. Phys. **87,** 1322 (2000).
24. J.-S. Chou and S.-C. Lee, J. Appl. Phys. **77,** 1805 (1995).
25. N. Nagai and H. Hashimoto, Appl. Surf. Sci. **172,** 307 (2001).
26. I. Shoten, Ed., *Iwanami Rikagaku Jiten (Iwanami's Physicochemical Dictionary)* (Tokyo, 1985), 3rd ed.
27. M. A. S. Kalceff and M. R. Phillips, Phys. Rev. B **52,** 3122 (1995).